Accurate Determination of the Absolute Quantum Yield for $O(^1D)$ Formation in the Photolysis of Ozone at 308 nm

Kenshi Takahashi,* Shinsuke Hayashi, Takayuki Suzuki, and Yutaka Matsumi

Solar-Terrestrial Environment Laboratory and Graduate School of Science, Nagoya University, Honohara 3-13, Toyokawa, Aichi, 442-8507, Japan

Received: July 12, 2004; In Final Form: September 3, 2004

Absolute $O(^1D)$ quantum yield from the photodissociation reaction of O_3 at 308 nm should be determined accurately with high precision for its atmospheric significance. This is because it has been used as a reference in previous relative measurements to obtain the $O(^1D)$ quantum yields as a function of photolysis wavelength in the near-UV region. In this study, the near-UV pulsed-laser photolysis of O_3 with the direct detection of the $O(^1D)$ and $O(^3P)$ photofragments using a technique of vacuum UV laser-induced fluorescence has been applied to determine the absolute $O(^1D)$ quantum yield from O_3 photolysis. The absolute $O(^1D)$ quantum yield at 308.0 nm at room temperature (298 ± 2 K) is determined to be 0.804 ± 0.048 (95% confidence interval), in which the uncertainty is much smaller than the values recommended for use in atmospheric studies. The $O(^1D)$ quantum yield values at photolysis wavelengths between 307 and 311.5 nm are also presented.

Introduction

In the near-ultraviolet (UV) region, O_3 dissociates into atomic and molecular oxygen through five energetically allowed channels:

$$O_3 + h\nu \rightarrow O(^1D) + O_2(a^1\Delta_g) \quad (\lambda < 309\ \text{nm}) \tag{1}$$

$$\rightarrow O(^3P) + O_2(X^3\Sigma_g^-) \quad (\lambda < 1180\ \text{nm}) \tag{2}$$

$$\rightarrow O(^1D) + O_2(X^3\Sigma_g^-) \quad (\lambda < 411\ \text{nm}) \tag{3}$$

$$\rightarrow O(^3P) + O_2(b^1\Sigma_g^+) \quad (\lambda < 463\ \text{nm}) \tag{4}$$

$$\rightarrow O(^3P) + O_2(a^1\Delta_g) \quad (\lambda < 612\ \text{nm}) \tag{5}$$

The long wavelength limits given in parentheses indicate the thermodynamic threshold for each channel.[1] From the viewpoint of atmospheric chemistry, the $O(^1D)$ atom is the most important species among the photoproducts. OH radicals in the stratosphere and troposphere and NO molecules in the stratosphere are produced from the reactions of $O(^1D)$ with H_2O and N_2O, respectively:

$$O(^1D) + H_2O \rightarrow 2OH \tag{6}$$

$$O(^1D) + N_2O \rightarrow 2NO \tag{7}$$

The reactive species created by these reactions, OH and NO, are immensely important in atmospheric chemistry. OH radicals initiate the atmospheric degradation of most natural and anthropogenic emissions entering the atmosphere. NO is a crucial ingredient of the stratosphere. Therefore, the quantum yield for $O(^1D)$ production in the UV photolysis of ozone is a key input for modeling calculations in atmospheric chemistry.[2,3]

Here, we call the probability of the formation of an $O(^1D)$ atom in the photolysis of an O_3 molecule at a given photolysis wavelength as $O(^1D)$ quantum yield. Photolysis rate of O_3 in the atmosphere is determined by the product of its absorption cross-section and the sunlight intensity. The sunlight spectral intensity below 300 nm is negligible in the troposphere and lower stratosphere, while the optical absorption cross-section of O_3 above 330 nm is negligibly small. Thus, the $O(^1D)$ quantum yields between 300 and 330 nm are of the most atmospheric significance.

There have been extensive experimental studies on the $O(^1D)$ quantum yield from O_3 photolysis of O_3 as a function of wavelength around 300−330 nm.[3,4] Most of them measured relative values of the $O(^1D)$ quantum yield at various photolysis wavelengths. To determine the absolute yield values from the relative measurements, a standard absolute yield value at a specific wavelength is required, and the $O(^1D)$ quantum yield at 308 nm has been utilized as the standard in many studies. There are only a few reports on the absolute $O(^1D)$ quantum yield measurements in this wavelength region.[5−8] Additional work to more accurately determine the absolute value of $O(^1D)$ quantum yield in this wavelength region has been needed, because the standard value affects the overall accuracy of the yields at other wavelengths.

In this paper, we report an experimental study to determine the absolute $O(^1D)$ quantum yield from O_3 photolysis at 308.0 nm at room temperature (298 ± 2 K). Both $O(^1D)$ and $O(^3P)$ atoms have been directly detected using a technique of vacuum ultraviolet laser-induced fluorescence (VUV-LIF). By treating the VUV-LIF intensities carefully, the absolute quantum yield value at 308.0 nm has been determined with reduced uncertainty as compared to the former studies. The $O(^1D)$ quantum yield values at photolysis wavelengths between 307 and 311.5 nm are also determined. Results are compared with the previously reported values and the current NASA/JPL recommendation[9] for use in atmospheric modeling.

Experimental Section

The experimental setup used in this study was almost the same as that in our previous studies of O_3 photochemistry.[6,7]

10.1021/jp0469259 CCC: $27.50
Published on Web 11/02/2004

We present only a brief description pertinent to the current study here. Both $O(^1D)$ and $O(^3P)$ photofragments produced in the UV photolysis of O_3 were probed using the VUV-LIF technique. The probe laser beams for the $O(3s^1D^\circ-2p^1D)$ and $O(3s^3S^\circ-2p^3P_j)$ transitions at $\lambda \approx 115$ and 130 nm, respectively, were generated by nonlinear frequency conversion processes in Xe/Ar or Kr. For the 115-nm generation, the phase-matched frequency-tripling scheme was achieved by focusing the UV photons (345 nm) from an excimer laser pumped-dye laser into a cell containing Xe/Ar mixture (10 Torr/200 Torr).[10] For the 130-nm generation, the VUV laser light was generated by a four-wave differential mixing scheme, $\omega_{VUV} = 2\omega_1 - \omega_2$, in Kr gas.[11] Two dye lasers were pumped by a single excimer laser (Lambda Physik, Compex 201, Scanmate 2E and FL3002E). Output from the first dye laser was frequency-doubled in a β-barium borate (BBO) crystal to generate 212.56 nm which is resonant to the two-photon transition of Kr. The wavelength of the other dye laser for the detection of $O(^3P_2)$ atoms was about 578 nm. Both laser outputs were overlapped using a dichroic mirror and focused into the cell containing Kr (20 Torr). The VUV photons at 115 or 130 nm were introduced into a reaction chamber through an LiF window that separated the rare gas cell and the reaction chamber. The VUV radiation collinearly counterpropagated with the photolysis beam in the reaction chamber. A part of the generated VUV photons was reflected into a photoionization cell containing 3 Torr of NO by a thin LiF plate. By monitoring the photoionization current from the NO cell, relative intensity variations of the VUV laser were measured.

The photolysis laser beam, being tunable between 307 and 311.5 nm, was obtained by frequency-doubling of the fundamental output from an Nd:YAG pumped-dye laser (Lambda Physik, Scanmate 2C-400) in a KD*P crystal. A mixture of two dyes (DCM and Sulforhodamin 640) in methanol solvent was used in the dye laser to obtain the photolysis radiation so that its intensity was almost constant between 614 and 628 nm. A color glass filter (Toshiba, UV-D33S) was inserted in the beam path to separate the fundamental and UV output. The bandwidth of the UV radiation was ~ 0.3 cm^{-1} (fwhm). The time delay between the photolysis and probe laser pulses was controlled by a pulse generator (Stanford Research, DG535) and was typically set to be 100 ns. The LIF signal was detected along the vertical direction, orthogonal to the propagation direction of both the photolysis and probe laser beams, by a solar-blind photomultiplier tube (EMR, 541J-08-17). The fluorescence detection direction was parallel to the electric vector of the photolysis laser and perpendicular to that of the probe laser. This photomultiplier tube was equipped with a LiF window and a KBr photocathode and is sensitive only in the wavelength range 106−150 nm. The output from the photomultiplier was accumulated using a gated integrator (Stanford Research, SR-250) over ten photolysis laser shots and stored on a personal computer. The detection limits of our VUV-LIF detection system for $O(^1D)$ and $O(^3P)$ were estimated to be on the order of 10^9-10^{10} atoms cm^{-3}.

The O_3 gas was produced by passing ultrapure O_2 (Nagoya Kosan, 99.9995%) through an ozonizer. The reaction chamber was evacuated by a rotary pump, and a mixture of O_3/He was slowly fed into the chamber through a poly(tetrafluoroethylene) needle valve. The total pressure in the chamber was maintained at 1.5 Torr and the partial pressure of O_3 was approximately 10 mTorr. The total pressure was measured by a capacitance manometer (MKS, Baratron 220) during the experiments. It should be noted that the high sensitivity of the VUV-LIF technique allows detection of $O(^1D)$ and $O(^3P_j)$ atoms at such low pressures and short pump−probe delay times and that secondary reactions of $O(^1D)$ and $O(^3P)$ can be ignored. For example, the room-temperature rate constant for the $O(^1D) + O_2$ reaction was reported to be $(3.8-4.18) \times 10^{-11}$ cm^3 molecule^{-1} s^{-1} at 298 K.[9,12−14] Formation of $O(^3P_j)$ atoms through this reaction did not interfere with the measurements of the $O(^3P)$ yield. The helium buffer gas used in these experiments is an inefficient quencher of $O(^1D)$[15] and has a negligible effect on the detection of $O(^1D)$ under our experimental conditions. The photolysis laser wavelength was monitored with a wavemeter (Burleigh, WA-4500).

We checked the photolysis laser power dependence of the LIF signal of $O(^1D)$ and $O(^3P)$ atoms. It was found that the $O(^1D)$ and $O(^3P)$ LIF signal intensities were linearly dependent on the photolysis laser power. The photolysis laser power for the spectral measurements was typically 0.3 mJ/pulse. The approximate fraction of photodissociated ozone molecules was estimated to be about 1% in the photodissociation zone under our experimental conditions. During the experiments, the photolysis laser power was monitored on a shot-by-shot basis using a pyroelectric laser power meter (Molectron, J4-09). The photolysis laser power did not vary much (<10%) as a function of wavelength between 306 and 314 nm.

Results

The ratios for both $O(^1D)$ and $O(^3P_2)$ LIF intensities at seven photolysis wavelengths (307, 308.5, 309, 309.5, 310, 310.5, and 311.5 nm) relative to those at 308 nm were measured. The photolysis laser wavelengths were alternatively changed between each of the seven wavelengths and 308 nm, while monitoring the $O(^1D)$ and $O(^3P_2)$ LIF at 115.22 and 130.22 nm, respectively. For the LIF intensity ratio measurements, several sets of experimental runs were performed at each photolysis wavelength. As indicated in our previous studies on the photolysis of O_3,[6,7] the populations of $O(^3P_j)$ among the spin−orbit states were measured by recording the fluorescence excitation spectra using the transitions of $3s^3S^\circ-2p^3P_j$ around 130 nm at the photolysis wavelengths stated already. No remarkable dependence of the j-populations on the photolysis wavelength was observed within the measurement uncertainties. Thus, the total $O(^3P_j)$ yield at various wavelengths is proportional to the LIF intensity of $O(^3P_2)$. For $O(^3P_j)$ photofragments, the translational energy is partly relaxed under our experimental conditions. The Doppler broadening of the resonance line of the $O(3s^3S^\circ-2p^3P_2)$ transition at 130.22 nm has been measured at all photolysis wavelengths studied here. No obvious dependence of the broadening on the photolysis wavelength was observed, which is consistent with our previous reports.[6,7] For $O(^1D)$ photofragments, little translational energy release was observed, because the $O(^1D) + O_2(a^1\Delta_g)$ pathway, which has a thermochemical threshold wavelength of 309.45 nm, is mainly responsible for $O(^1D)$ formation in the photolysis wavelength range studied here.[3,4] No obvious dependence of the line profiles on the photolysis wavelength was observed, which is consistent with our previous reports.[6,7]

The near-UV absorption spectrum of O_3 does not show any features narrower than ~ 0.1 nm even at low temperature,[16] indicating that the photoexcited states have extremely short lifetimes due to photodissociation processes. The atomic products in the photolysis of O_3 must be $O(^1D)$ and/or $O(^3P)$ at wavelengths longer than 234 nm, which is the thermochemical threshold for production of the second-lowest electronically

TABLE 1: Ratios of the O(^{1}D) and O(^{3}P) LIF Intensities at Wavelengths between 307 and 311.5 nm, Relative to Those at 308 nm, in the Photolysis of O_3 at Room Temperature (298 ± 2 K) and Absorption Cross-section Ratios of O_3

λ (nm)[a]	$R_{1D}(\lambda_i)$[b]	$R_{3P}(\lambda_i)$[c]	$R_{abs}(\lambda_i)$[d]
307.0	1.200 ± 0.094	0.981 ± 0.048	1.138
308.0	1	1	1
308.5	0.867 ± 0.080	1.302 ± 0.068	0.942
309.0	0.773 ± 0.084	1.498 ± 0.080	0.912
309.5	0.644 ± 0.064	1.665 ± 0.140	0.795
310.0	0.495 ± 0.064	1.829 ± 0.084	0.749
310.5	0.414 ± 0.088	1.921 ± 0.128	0.708
311.5	0.289 ± 0.046	2.156 ± 0.176	0.656

[a] Photolysis wavelength in nm. [b] Fluorescence intensity ratio for O(^{1}D). The quoted error bars include possible systematic and 2σ precision uncertainties in 10−16 measurements. See eq 9 in the text. [c] Fluorescence intensity ratio for O(^{3}P). The quoted error bars include possible systematic and 2σ precision uncertainties in 10−16 measurements. See eq 10 in the text. [d] Absorption cross-section ratio for O_3. See eq 11 in the text. The values are calculated from the absorption cross-section measured by Malicet et al.[15]

excited O(^{1}S) atom.[1] The photolysis quantum yield of O_3 should be unity in the UV absorption band around 300−320 nm

$$\Phi_{1D}(\lambda) + \Phi_{3P}(\lambda) = 1 \quad (8)$$

where $\Phi_{1D}(\lambda)$ and $\Phi_{3P}(\lambda)$ are the quantum yields for O(^{1}D) and O(^{3}P) formation from O_3 photolysis, respectively.

The ratios of the relative production yields for O(^{1}D) and O(^{3}P) at photolysis wavelengths λ_i (i = 1−7) to those at 308 nm, $R_{1D}(\lambda_i)$ and $R_{3P}(\lambda_i)$, were obtained from the observed LIF intensities which were normalized by the photolysis laser intensities. The ratio for O(^{1}D) formation was defined as follows;

$$R_{1D}(\lambda_i) \equiv \frac{\sigma_{abs}(\lambda_i)\Phi_{1D}(\lambda_i)}{\sigma_{abs}(308)\Phi_{1D}(308)} = \frac{F_{1D}(\lambda_i)I_p(308)}{F_{1D}(308)I_P(\lambda_i)}, \quad (9)$$

and for O(^{3}P) formation;

$$R_{3P}(\lambda_i) \equiv \frac{\sigma_{abs}(\lambda_i)\Phi_{3P}(\lambda_i)}{\sigma_{abs}(308)\Phi_{3P}(308)} = \frac{F_{3P}(\lambda_i)I_p(308)}{F_{3P}(308)I_P(\lambda_i)}, \quad (10)$$

where $\sigma_{abs}(\lambda_i)$ is the photoabsorption cross-section of ozone at λ_i, $I_p(\lambda_i)$ is the photolysis laser intensity at λ_i, and $F_{1D}(\lambda_i)$ and $F_{3P}(\lambda_i)$ are the LIF intensities of O(^{1}D) and O(^{3}P) at λ_i, respectively. The ratios of the photoabsorption cross-sections to that at 308 nm were also defined as

$$R_{abs}(\lambda_i) \equiv \frac{\sigma_{abs}(\lambda_i)}{\sigma_{abs}(308)} \quad (11)$$

The precise photoabsorption cross-sections of O_3 in the UV region at room temperature have been measured by three groups.[17−19] The $R_{abs}(\lambda_i)$ values derived from the three reports coincided with each other within less than 1% accuracy at seven wavelengths and 308 nm.

If we use $R_{1D}(\lambda_i)$, $R_{3P}(\lambda_i)$, and $R_{abs}(\lambda_i)$ in eqs 8−10, we obtain the following expression

$$R_{3P}(\lambda_i) - R_{abs}(\lambda_i) = \Phi_{1D}(308)[R_{3P}(\lambda_i) - R_{1D}(\lambda_i)] \quad (12)$$

The values of $R_{1D}(\lambda_i)$ and $R_{3P}(\lambda_i)$ obtained in this study are listed in Table 1. The values of $R_{abs}(\lambda_i)$ calculated from the absorption cross-sections of Malicet et al.[17] are also listed in Table 1. Figure 1 shows the plot of $R_{3P}(\lambda_i) - R_{abs}(\lambda_i)$ versus $R_{3P}(\lambda_i) - R_{1D}(\lambda_i)$, where the slope corresponds to the value of $\Phi_{1D}(308)$. On the basis of eq 12, we determined the value of $\Phi_{1D}(308)$ by the weighted least-squares fit analysis method. The obtained value of $\Phi_{1D}(308)$ is 0.804 ± 0.048 (95% confidence interval), in which the error includes possible systematic and statistical uncertainties. In the regression analysis, random errors in the fluorescence intensity and laser power measurements, the upper limit of the systematic error in the measurements (2%), and the upper limit of the errors in the absorption cross-section ratios (1%) are taken into account. The partial cross-sections $\sigma_{abs}(\lambda_i)\cdot F_{1D}(\lambda_i)$ and $\sigma(\lambda_i)\cdot F_{3P}(\lambda_i)$ versus the photolysis wavelength thus determined are plotted in Figure 2. The O(^{1}D) quantum yields at λ_i have also been determined, which are listed in Table 2. We have also calculated the $\Phi_{1D}(308)$ value using the absorption cross-section data reported by Molina and Molina[17] instead of those by Malicet et al.[18] The difference between the two results for the $\Phi_{1D}(308)$ value was negligibly small (<0.2%).

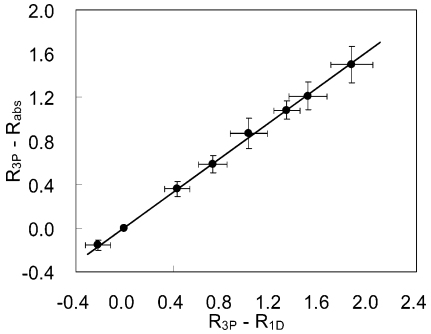

Figure 1. A plot of ($R_{3P} - R_{abs}$) vs ($R_{3P} - R_{1D}$) for the various photolysis wavelengths between 307 and 331.5 nm (see text). The wavelengths associated with each data point are given in Table 1. The slope of the plot corresponds to the absolute O(^{1}D) quantum yield at 308 nm. A straight line indicates the result of the weighted linear least-squares fit analysis of the experimental data.

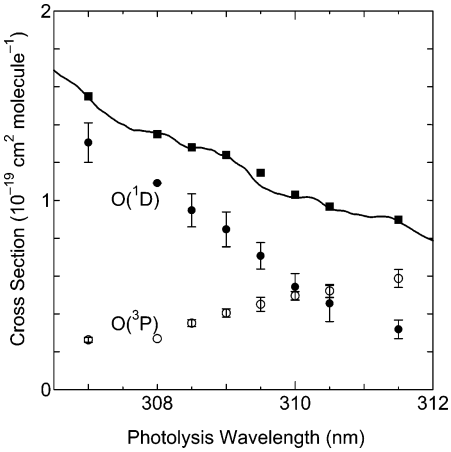

Figure 2. Partial cross-sections for the formation of O(^{1}D) and O(^{3}P) in the photolysis of O_3 and total photoabsorption cross-sections of O_3 as a function of photolysis wavelength. A solid curve indicates the absorption cross-sections of O_3 measured by Malicet et al.[18]. Filled (●) and open (○) circles indicate the partial cross-sections for the formation of O(^{1}D) and O(^{3}P), respectively, which were calculated from the relative fluorescence intensity measurements with the O(^{1}D) quantum yield of 0.804 at 308 nm. Filled squares (■) indicate the total cross-sections calculated from the partial cross-sections (see text). Error bars include systematic and 2σ precision uncertainty.

Discussion

In this study, the absolute quantum yield for O(^{1}D) production from O_3 photolysis at 308.0 nm at 298 ± 2 K has been determined to be $\Phi_{1D}(308) = 0.804 \pm 0.048$. Table 3 indicates

TABLE 2: $O(^1D)$ Quantum Yield from O_3 Photolysis in the Wavelength Range of 307−311.5 nm at 298 K

	$\Phi_{1D}(\lambda)^b$	
λ (nm)[a]	this work[c]	NASA/JPL recommendation[d]
307.0	0.848 ± 0.084	0.86 ± 0.09
308.0	0.804 ± 0.048	0.79 ± 0.08
308.5	0.740 ± 0.081	0.74 ± 0.07
309.0	0.682 ± 0.084	0.67 ± 0.07
309.5	0.613 ± 0.071	0.60 ± 0.06
310.0	0.531 ± 0.075	0.52 ± 0.05
310.5	0.470 ± 0.103	0.45 ± 0.05
311.5	0.354 ± 0.060	0.34 ± 0.04

[a] Photolysis wavelength in nm. [b] $O(^1D)$ quantum yield value at photolysis wavelength λ. [c] The error corresponds to 95% confidence intervals. [d] The error indicates ±10% (1σ) precision uncertainty, as noted by Sander et al.[9]

TABLE 3: Absolute Measurements of the Quantum Yield for $O(^1D)$ Production from O_3 Photolysis at 308 nm at Room Temperature

$\Phi_{1D}(\lambda)$	uncertainty	ref
0.804	± 0.048[a]	this work
0.79	± 0.10[b]	ref 8
0.79	± 0.12	ref 6
0.79[c]	± 0.02	ref 5

[a] The error bars correspond to the 95% confidence interval. [b] The error bars include systematic error and 2σ precision. [c] $k_{13}/k_{14} = 1.0$ was assumed.

the comparison of the value in this study with the previous measurements of $\Phi_{1D}(308)$ at room temperature. Our value is in good agreement with the previously reported values within the quoted uncertainties, while the uncertainty in our present study is reduced significantly. Talukdar et al.[8] and Greenblatt and Wiesenfeld[5] measured the time profile of $O(^3P)$ resonance fluorescence after the pulsed-laser photodissociation of O_3 at 308 nm at room temperature. The temporal profile of $O(^3P)$ initially jumps because of its direct formation in the photolysis of O_3, followed by an exponential rise controlled by the following reactions of $O(^1D)$ and a slow decay due to diffusion:

$$O(^1D) + O_3 \rightarrow 2O_2 \qquad k_{12} \tag{13}$$

$$O(^1D) + O_3 \rightarrow 2O(^3P) + O_2 \qquad k_{13} \tag{14}$$

On the basis of experimental results that the two rate coefficients are equal ($k_{13}/k_{14} = 1.0$),[8] the absolute $O(^1D)$ quantum yield was calculated from amounts of the initial jump and the exponential rise of the $O(^3P)$ signal. The uncertainty of the measurements for the $O(^1D)$ quantum yield using the time profile of $O(^3P)$ is directly affected by that of the rate constant ratio k_{13}/k_{14}. The value of the rate constant ratio has been reported to be $k_{13}/k_{14} = 1.0 \pm 0.1$ (2σ uncertainty).[8] This uncertainty for k_{13}/k_{14} results in the uncertainty of 10% in the $O(^1D)$ quantum yield value.

In our previous studies,[6,7] the photofragment yield spectra of both $O(^3P)$ and $O(^1D)$ atoms produced in the photolysis of O_3 were measured by scanning the photolysis laser wavelength between 305 and 329 nm while monitoring the LIF signal intensities of $O(^3P)$ and $O(^1D)$ using the VUV-LIF technique. The sum of those photofragment yield spectra with absolute scales should coincide to the absorption spectrum of O_3 molecule

$$\sigma_{abs}(\lambda) = s_{1D}Y_{1D}(\lambda) + s_{3P}Y_{3P}(\lambda) \tag{15}$$

where $Y_{1D}(\lambda)$ and $Y_{3P}(\lambda)$ are the experimentally obtained photofragment yield spectra of $O(^1D)$ and $O(^3P_j)$, and s_{1D} and s_{3P} are the detection sensitivity factors for $O(^1D)$ and $O(^3P_j)$, respectively. Pairs of s_{1D} and s_{3P} values were determined so that the sum of $s_{1D}Y_{1D}(\lambda)$ and $s_{3P}Y_{3P}(\lambda)$ could reproduce the absorption spectrum $\lambda_{abs}(\lambda)$. The absolute value of the $O(^1D)$ quantum yield is calculated as $\Phi_{1D}(\lambda) = s_{1D}Y_{1D}(\lambda)/[s_{1D}Y_{1D}(\lambda) + s_{3P}Y_{3P}(\lambda)]$. In our previous studies,[6,7] because of both the run-by-run fluctuations including systematic and random errors in the wavelength continuous spectra and fitting errors for determination of the sensitivity factors, the resultant values of the $O(^1D)$ quantum yield accompanied a 15% uncertainty between 305 and 329 nm. In the present study, we have focused on the accurate determination of $\Phi_{1D}(308)$. Clearly, the uncertainty of $\Phi_{1D}(308)$ is reduced in this study by measuring the fluorescence intensity ratios at seven wavelengths $R_{1D}(\lambda_i)$ and $R_{3P}(\lambda_i)$ repeatedly and by adopting the rigorous mathematical method described already (eqs 8−12) to determine the $\Phi_{1D}(308)$ value.

In most previous studies on the determination of the $O(^1D)$ quantum yields in the UV photolysis of O_3, the relative quantum yields have been measured, and the absolute $O(^1D)$ quantum yield value at 308 nm has been utilized as an anchor to obtain the $O(^1D)$ yield values as a function of photolysis wavelength.[20−23] The uncertainty of $\Phi_{1D}(308)$ is propagated to $\Phi_{1D}(\lambda)$ at other wavelengths in such relative measurements. Reduction of the uncertainty is essential for a precise estimation of the production rates of atmospheric radicals such as HO_x. The chemical reaction between the $O(^1D)$ produced from UV photolysis of O_3 and H_2O provides an important source of atmospheric OH radicals.[2] Precise estimation of OH production rates is crucial for determining atmospheric lifetimes of atmospheric molecules such as CH_4, CO, and natural and anthropogenic hydrocarbons, because OH is a strong oxidizer, and thus, the reactions of OH with those constituents proceed very efficiently in the troposphere and stratosphere. Furthermore, intercomparison studies of chemical actinometers and spectroradiometers measuring $j(O(^1D))$ are clearly dependent on the accurate and precise laboratory determination of the $O(^1D)$ quantum yield.[24,25]

Acknowledgment. The financial support for this work by Grants-in-Aid from the Ministry of Education, Culture, Sports, Science and Technology, Japan, is greatly acknowledged. The financial support by the Sumitomo Foundation is also gratefully acknowledged.

References and Notes

(1) Atkinson, R.; Baulch, D. L.; Cox, R. A.; Hampson, R. F., Jr.; Kerr, J. A.; Rossi, M. J.; Troe, J. *J. Phys. Chem. Ref. Data* **1997**, *26*, 521.

(2) Brasseur, G. P.; Orlando, J. J.; Tyndall, G. S. *Atmospheric Chemistry and Global Change*; Oxford University Press: New York, 1999.

(3) Matsumi, Y.; Kawasaki, M. *Chem. Rev.* **2003**, *103*, 4767.

(4) Matsumi, Y.; Comes, F. J.; Hancock, G.; Hofzumahaus, A.; Hynes, A. J.; Kawasaki, M.; Ravishankara, A. R. *J. Geophys. Res.* **2002**, *107*, 4024.

(5) Greenblatt, G. D.; Wiesenfeld, J. R. *J. Chem. Phys.* **1983**, *78*, 4924.

(6) Takahashi, K.; Matsumi, Y.; Kawasaki, M. *J. Phys. Chem.* **1996**, *100*, 4084.

(7) Takahashi, K.; Taniguchi, N.; Matsumi, Y.; Kawasaki, M.; Ashfold, M. N. R. *J. Chem. Phys.* **1998**, *108*, 7161.

(8) Talukdar, R. K.; Gilles, M. K.; Battin-Leclerc, F.; Ravishankara, A. R.; Fracheboud, J. M.; Orlando, J. J.; Tyndall, G. S. *Geophys. Res. Lett.* **1997**, *24*, 1091.

(9) Sander, S. P.; Friedl, R. R.; Golden, D. M.; Kurylo, M. J.; Huie, R. E.; Orkin, V. L.; Moortgat, G. K.; Ravishankara, A. R.; Kolb, C. E.; Molina, M. J.; Finlayson-Pitts, B. J. *Chemical Kinetics and Photochemical Data for Use in Atmospheric Studies*, Evaluation No. 14; Publication JPL 02-25; Jet Propulsion Laboratory, California Institute of Technology: Pasadena, CA, revised Feb. 2003.

(10) Hilbig, R.; Wallenstein, R. *Appl. Opt.* **1982**, *21*, 913.

(11) Marangos, J. P.; Shen, N.; Ma, H.; Hutchinson, M. H. R.; Connerade, J. P. *J. Opt. Soc. Am. B* **1990**, *7*, 1254.

(12) Strekowski, R. S.; Nicovich, J. M.; Wine, P. H. *Phys. Chem. Chem. Phys.* **2004**, *6*, 2145.
(13) Dunlea, E. J.; Ravishankara, A. R. *Phys. Chem. Chem. Phys.* **2004**, *6*, 2152.
(14) Blitz, M. A.; Dillon, T. J.; Heard, D. E.; Pilling, M. J.; Trought, I. D. *Phys. Chem. Chem. Phys.* **2004**, *6*, 2162.
(15) Heidner, R. F., III; Husain, D. *Int. J. Chem. Kinet.* **1974**, *6*, 77.
(16) Freeman, D. E.; Yoshino, K.; Esmond, J. R.; Parkinson, W. H. *Planet. Space Sci*. **1984**, *32*, 239.
(17) Molina, L. T.; Molina, M. J. *J. Geophys. Res.* **1986**, *91*, 14501.
(18) Malicet, J.; Daumont, D.; Charbonnier, J.; Parisse, C.; Chakir, A.; Brion, J. *J. Atmos. Chem.* **1995**, *21*, 263.
(19) Voigt, S.; Orphal, J.; Bogumil, K.; Burrows, J. P. *J. Photochem. Photobiol., A* **2001**, *143*, 1.
(20) Hancock, G.; Tyley, P. L. *Phys. Chem. Chem. Phys.* **2001**, *3*, 4984.
(21) Smith, G. D.; Molina, L. T.; Molina, M. J. *J. Chem. Phys.* **2000**, *A104*, 8916.
(22) Bauer, D.; D′Ottone, L.; Hynes, A. J. *Phys. Chem. Chem. Phys.* **2000**, *2*, 1421.
(23) Talukdar, R. K.; Longfellow, C. A.; Gilles, M. K.; Ravishankara, A. R. *Geophys. Res. Lett.* **1998**, *25*, 143.
(24) Cantrell, C. A.; Calvert, J. G.; Bais, A.; Shetter, R. E.; Lefer, B. L.; Edwards, G. D. *J. Geophys. Res.* **2003**, *108*, 8542.
(25) Hofzumahaus, A.; Lefer, B. L.; Monks, P. S.; Hall, S. R.; Kylling, A.; Mayer, B.; Shetter, R. E.; Junkermann, W.; Bias, A.; Calvert, J. G.; Cantrell, C. A.; Madronich, S.; Edwards, G. D.; Kraus, A.; Müller, M.; Bohn, B.; Schmitt, R.; Johnston, P.; McKenzie, R.; Frost, G. J.; Griffioen, E.; Krol, M.; Martin, T.; Pfister, G.; Röth, E. P.; Ruggaber, A.; Swartz, W. H.; Lloyd, S. A.; Van Weele, M. *J. Geophys. Res.* **2004,** *109*, D08S90, doi: 10.1029/2003JD004333.